INTERNATIONAL JOURNAL OF HYDROGEN ENERGY 42 (2017) 9003–9010

Available online at www.sciencedirect.com

ScienceDirect

journal homepage: www.elsevier.com/locate/he

Effect of under nitrogen annealing on photo-electrochemical characteristics of films deposited from authentic Cu_2SnSe_3 sources by thermal vacuum under argon gas condensation

Nordin Sabli [a,b,*], *Zainal Abidin Talib* [c], *Hikmat S. Hilal* [d]

[a] *Department of Chemical and Environmental Engineering, Faculty of Engineering, Universiti Putra Malaysia, 43400, UPM Serdang, Selangor, Malaysia*

[b] *Institute of Advance Technology (ITMA), Universiti Putra Malaysia, 43400, UPM Serdang, Selangor, Malaysia*

[c] *Department of Physics, Faculty of Science, Universiti Putra Malaysia, 43400, UPM Serdang, Selangor, Malaysia*

[d] *SSERL, Department of Chemistry, An-Najah N. University, Nablus, West Bank, Palestine*

ARTICLE INFO

Article history:
Received 30 October 2015
Received in revised form
21 April 2016
Accepted 21 April 2016
Available online 20 May 2016

Keywords:
Argon gas condensation
Thermal evaporation
Photoelectrochemical characteristics
Photoactivity
Copper tin selenide film

ABSTRACT

This communication describes how annealing under nitrogen affects photo-electrochemical characteristics of films deposited from authentic Cu_2SnSe_3 sources by vacuum evaporation under argon gas (low flow rate 5 cm^3/min) using substrate 300 °C. Annealing lowered the photoresponse of the deposited film, by affecting crystallite structure, morphology, composition and pores in the films. Annealing at temperatures in the range 150–350 °C improved crystallinity of the film but lead to pore formation between adjacent, which lowered photoresponse by increased resistance across the electrode/redox interface. Higher temperature (450 °C) annealing lead to SnO_2 formation, as an additional phase, at the expense of Cu_2SnS_3 decomposition. Porosity and mixed phases with SnO_2 presumably increased film internal resistance and resulted in poor charge transfer across the solid/redox couple interface. By affecting film characteristics, annealing lowered photoresponse for the deposited films.

Introduction

Metal chalcogenide based films have medium band gap values, and absorb in the visible light, which makes them potentially useful materials in modern technology [1]. Annealing is a technique that is widely used to enhance characteristics of different materials, and thin films are no exclusion. Treatment of thin films by annealing is widely practiced to improve their structure and morphology. Annealing a thin film may enhance its optical, electrical, magnetic and photo-electrochemical characteristics [2–6]. Moreover, controlling annealing conditions is necessary in thin film technology. Some materials are not stable to high annealing temperatures and may undergo unwanted

* *Corresponding author*. Department of Chemical and Environmental Engineering, Faculty of Engineering, Universiti Putra Malaysia, 43400, UPM Serdang, Selangor, Malaysia.
E-mail address: nordin_sab@upm.edu.my (N. Sabli).

http://dx.doi.org/10.1016/j.ijhydene.2016.04.155

chemical changes by over heat [7,8]. Highly stable materials, such as TiO_2 and Al_2O_3, can be annealed at temperatures above 600 °C and under oxygen. Other materials with lower stability should be annealed only at moderate temperatures with the exclusion of oxygen. Commonly speaking, materials with wide band gaps are more stable than those with narrower band gaps [9].

Ternary metal tin chalcogenide film electrodes attract attention due to their potential to be used as non-linear optical and solar cell materials. Earlier reports described preparation of Cu_2SnSe_3 by vacuum evaporation [10–12]. Talib et al. [10] prepared Cu_2SnSe_3 films onto glass substrates at room temperature by vacuum thermal evaporation using directly mixed powder of copper, tin and selenium in stoichiometric ratio (2:1:3) as a source. The resulting as-deposited and annealed films involved two phases of Cu_2SnSe_3 and SnSe. Babu et al. [11] prepared Cu_2SnSe_3 films onto glass substrates by a three-source co-evaporation technique from pure elements of copper, tin and selenium. After film deposition, the in-situ post-deposition under selenium atmosphere was carried out by heating the substrate at a temperature of 500 °C for about 45 min to obtain Cu_2SnSe_3 film. Bhaskar et al. [12] prepared Cu_2SnSe_3 films onto glass substrates at 300 °C by co-evaporation technique. The as-deposited Cu_2SnSe_3 films involved SnSe as a secondary phase which disappeared on annealing under selenium atmosphere at 500 °C for an hour. Talib et al. studied the effect of annealing temperature under nitrogen gas for Cu_2SnSe_3 films prepared by vacuum evaporation of the elemental forms of Cu, Sn and Se mixed together in one crucible, and the mixture was then used as a source material for the deposited films [10,13]. The technique involved the difficulty of different melting points for the different elements which made it difficult to control resulting film composition. Due to different melting points the elements evaporated at different rates at the same temperature. Therefore, annealing was necessary to homogenize the resulting films.

In a more recent report, we prepared films by vacuum evaporation using authentic Cu_2SnSe_3 as a source material under different deposition conditions, including argon gas flow rate, substrate temperature and other factors [14]. The report mentioned that annealing lowered photoresponse of the deposited film, but the issue was not studied therein. The report did not discuss why or how annealing may lower photoresponse, nor did it show the effect of annealing on film crystallinity, morphology, particle size or composition. It is imperative to know how annealing may affect film photoresponse. The new submission is focused on these issues.

The main goal of this new work is to investigate the effect of annealing, under a nitrogen stream, on photoresponse of films deposited from authentic Cu_2SnSe_3 films. This work will answer the following questions: Does annealing (and annealing temperature) affect the film electrode photoresponse? If yes, how and why? Is it due to change in composition, morphology and/or particle size? To our knowledge, no similar studies have been reported. The study will conclude with recommendations on the feasibility of annealing the films under nitrogen atmosphere.

Experimental section

Chemicals

Potassium hexacyanoferrate (III), $K_3[Fe(CN)_6]$ and potassium hexacyanoferrate(II) trihydrate, $K_4[(Fe(CN)_6)].H_2O$ were purchased from Sigma Aldrich. Hydrochloric acid, HCl was purchased from Friendmann Schmidt Chemical. Organic solvents, methanol and 2-propanol, were purchased from Merck KGaA and HmbG Chemicals respectively. Starting materials copper, tin and selenium were all purchased from Alfa Aesar with nominal purity 99.8, 99.5 and 99.5% respectively.

Film electrode preparation

The Cu_2SnSe_3 alloy source material was prepared using the melt-quenching method [15]. The powders of copper, tin and selenium were weighed according to nominal stoichiometric 2:1:3 molar ratios, mixed, sealed in a vacuum quartz ampoule and heated. The Cu_2SnSe_3 resulting compound was taken out of the ampoule, ground into fine powder and made ready for XRD analysis. After confirming its structure by XRD, the prepared compound powder was then used as source material.

The Cu_2SnSe_3 powder (0.10 g) was placed in a molybdenum evaporation boat. In order to obtain strong adherence and film uniformity, substrates of highly conductive ITO/glass slides, were cleaned prior to deposition. The multi-step cleaning process involved washing with a detergent, rinsing with distilled water, washing with methanol, rinsing again with distilled water, soaking in dilute HCl 10% (v/v) for 10 s, rinsing with distilled water, washing with methanol, rinsing again with distilled water and rinsing with boiling isopropyl alcohol before drying.

The substrates were mounted on a mask that was placed 14 cm above the boat. The system was then covered with a bell jar and evacuated to a pressure of 5×10^{-4} Pa. A heater was kept directly above the substrate, and a thermocouple was used to monitor the substrate temperature. Substrate heating was intentionally performed to improve film adhesion, increase surface mobility of condensing atoms and enhance crystallinity, as described earlier [16]. Substrate heating is also necessary for the reaction of metal and chalcogen atoms adsorbed therein [17]. The substrate temperature (300 °C) was used here based on earlier studies [12] to deposit Cu_2SnSe_3 films.

The argon gas was introduced into the vacuum chamber via an inlet tube having a nozzle 0.5 mm in diameter at a flow rate $V_A = 5$ cm^3/min. The nozzle was mounted near the evaporation boat, and its outlet direction was pointed towards the substrate. Prior to deposition, the boat containing the Cu_2SnSe_3 powder was pre-heated for 1 h at a temperature lower than the melting point (<900 °C). By gradually increasing the applied current, the Cu_2SnSe_3 powder melted, evaporated from the boat and deposited on the substrate, which was kept at 300 °C during the evaporation process. At the end, heating was stopped and the films were allowed to cool to room temperature under vacuum/Argon gas. The films were then taken and stored in a desiccator.

Film electrode annealing

Film annealing was performed in the same deposition apparatus described above, at different temperatures of (T_A = 150, 250, 350 and 450 °C) under atmospheric pressure of pure nitrogen gas (99.999%) for 30 min. The heating ramp rate was 5 °C/min. After the desired annealing temperature was achieved, the film was left for 30 min. Heating was then stopped under continuous flow of nitrogen to cool down at a rate of 5 °C. The annealed samples were taken and stored in a desiccator for further use.

Film electrode characterization

As-deposited and annealed film thickness values were measured using an Ambious-Tech XP-200 high resolution surface profilometer. The film thickness values were 143, 325, 275, 38 and 34 nm for films annealed at room temperature (un-annealed), 150, 250, 350 and 450 °C, respectively.

The XRD patterns were measured on an XPERT-PRO X-ray diffractometer with Cu K_α [1.54056 Å]. The atomic compositions of the films were investigated by EDX (Oxford Instruments model 7353) attached to a Nova NanoSEM 230 field emission scanning electron microscope (FESEM) which was also used to study surface morphology.

PEC experiments

PEC experiments were performed using the $[Fe(CN)_6]^{-3}$ (0.05 M)/$[Fe(CN)_6]^{-4}$ (0.05 M) redox system, by running linear sweep voltammetry in the range +1.0 V and −1.0 V with a scan speed of 20 mV/s using a PGSTAT 101 Potentiostat. A conventional three-electrode cell, equipped with a platinum counter electrode and an Ag/AgCl reference electrode, was used. An Osram halogen lamp was used as a light source. The light intensity at the working electrode was measured by a pyranometer (LI-200; Li-Cor, USA) to be 0.1 W/cm^2 and used to directly illuminate the sample. The light was intermittently chopped on and off by a thick black cardboard at 0.5 cycles per second to give the effects of photocurrent and dark current.

Results and discussion

X-ray diffraction

Effect of annealing temperature on deposited film structure was studied using XRD. Fig. 1 shows XRD patterns for JCPDS references, ITO/glass substrate, Cu_2SnSe_3 source powder and films annealed at different temperatures. Cu_2SnSe_3 powder peaks were compared with JCPDS Card number 98-007-7744 and indexed. The presence of the ITO peaks in the patterns is widely observed in thin films deposited by different methods [12–16]. Films with high thickness do not show ITO peaks. The XRD patterns confirmed the formation of polycrystalline Cu_2SnSe_3 with the plane (002)/(13-1) being the strongest orientation. The diffraction peaks from (33-1)/(060), (262)/(40-4) planes were clearly observed. The peaks were well-matching with the JCPDS Card. The XRD patterns recorded for the deposited films, prepared from Cu_2SnSe_3 powder,

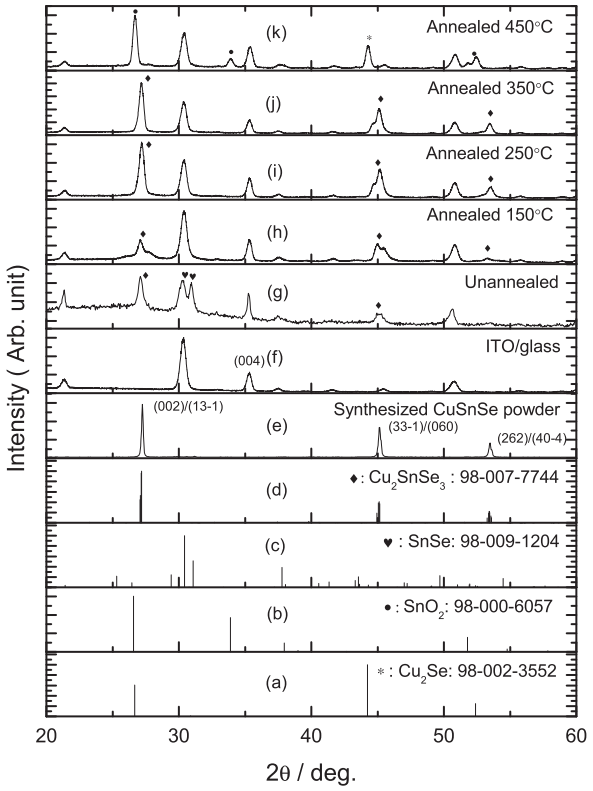

Fig. 1 – XRD patterns for JCPDS references, CuSnSe source powder, ITO/glass substrate and films annealed at different temperatures (T_A): (a) un-annealed (b) 150, (c) 250, (d) 350 and (e) 450 °C.

under different annealing temperatures, are shown in Fig. 1g–k. The prominent Bragg reflections at (or around) 2θ = 27.1° corresponding to (002)/(13-1) diffraction planes belong to Cu_2SnSe_3 (Fig. 1g–j). The Cu_2SnSe_3 three peaks in the un-annealed film (Fig. 1g) are consistent with those observed for authentic Cu_2SnSe_3 compound shown in Fig. 1d. Fig. 1g also shows the presence of SnSe phase, as compared with the authentic SnSe phase in (Fig. 1c). The broad hump background observed in Fig. 1g, for un-annealed film, was overcome by annealing. There were no observed SnSe peaks in films annealed at temperatures in the range 150–350 °C. The Cu_2SnSe_3 three prominent peaks could be observed more clearly at higher annealing temperatures in that range, Fig. 1h–j. This indicates the enhanced crystallinity and purity of the films annealed in the range 150–350 °C, which confirms the added value of annealing Cu_2SnSe_3 film electrodes under these conditions.

The three prominent peaks, belonging to Cu_2SnSe_3, as observed in Fig. 1d, disappeared by annealing at 450 °C (Fig. 1k). At high annealing temperature, the Cu_2SnSe_3 compound decomposed. Fig. 1k shows three new peaks at (or around) 2θ = 27.2°, 33.9° and 52.4° corresponding to (110), (011) and (121) diffraction planes, respectively. The peaks correspond to those of the authentic SnO_2 compound as shown in Fig. 1b. Prominent Bragg reflection peak at (or around) 2θ = 44.3° corresponding to the authentic Cu_2Se (Fig. 1a) was also observed in Fig. 1k. The XRD patterns show that at higher annealing temperature 450 °C, the Cu_2SnSe_3 compound in the

film decomposed and produced a new SnO_2 phase. The Figure also shows the production of SnSe as compared to authentic SnSe in Fig. 1c. Although annealing was conducted under inert gas (nitrogen gas) atmosphere which means no oxygen was supplied, the formation of SnO_2 phase could be explained due to the traces of impurities in the nitrogen gas (99.999% pure). The nitrogen gas still contains moisture (3 ppm), oxygen (3 ppm) and carbon monoxide (1 ppm) that can be sources of oxygen during annealing, *vide infra*.

Film crystallinity was studied by calculating the ratio between the peaks for Cu_2SnSe_3 films (002)/(13-1) and the ITO/glass (004) as a reference. The higher ratios between peak intensities of the Cu_2SnSe_3 (002)/(13-1) and ITO/glass (004) could be due to higher crystallinity for Cu_2SnSe_3, as discussed in more depth below Earlier literature showed similar analysis for other different films [18,19]. Crystallinity of film annealed at 450 °C could not be similarly discussed as the film did not involve significant amount of Cu_2SnSe_2 compound. Table 1 summarizes values of peak intensity ratios for films annealed at different temperatures. A trend of increase in ratio with higher temperature in the range 150 °C–350 °C could be clearly observed. The Table shows that the films annealed at 250 °C and above exhibited higher crystallinity. The ratio could be due to more than one factor, namely film thickness, composition, compactness and crystallinity. The fact that the films annealed at 150, 250 and 350 °C have similar composition, and the film annealed at 350 °C has lowest thickness in the series (38 nm) with highest ratio indicates that it has highest crystallinity and compactness among the annealed films. Moreover, the film annealed at 250 °C is thinner than that annealed at 150 °C, but still has higher ratio, which means that it has higher compactness and crystallinity. More discussion on film crystallinity, particle size and compactness will be presented in Section 3.2 below.

Collectively, the XRD results confirm that annealing the Cu_2SnSe_3 films in the range 150–350 enhances their crystallinity and purity.

Scanning electron microscopy

Surface morphology for un-annealed and annealed films was studied using SEM. Fig. 2 shows the SEM images of films deposited at different annealing temperatures. The Figure shows that un-annealed film morphology was affected by annealing. Moreover, different annealing temperatures have different effects on morphology. The SEM results are thus consistent with XRD results discussed above.

The SEM micrograph of the un-annealed film shows a mixture of particles with no uniform shapes or sizes, Fig. 2a. Larger particles (of up to 100 nm) with sharp edges can be observed together with smaller round shaped particles of less than 20 nm. The mixed particle SEM shapes could be an indication of mixed phases, as described by the XRD results above. Earlier literature showed that films with mixed phases have mixed particle shapes [20].

Annealing the films at temperatures in the range 150–350 °C yielded more uniform rod shaped particles with clear sharp edges, Fig. 2b–d. The absence of the smaller round shaped particles in the annealed films is consistent with the lower content of the SnSe phase as discussed by the XRD results above. Moreover, the annealed films involve larger particles (~100 nm in width and more than 200 nm in length) than those in the un-annealed film. Typically, larger particles have lower relative surface areas and less relative surface atoms than smaller particles. Therefore, the XRD patterns for nanoparticles have shorter and wider peaks than their bulk material counterparts [19,21]. The enhanced morphology and increased particle sizes in the annealed films, as observed by SEM micrographs, are thus consistent with the XRD patterns discussed above.

The fact that annealing the particles affects their sizes and composition is known for other different nano-size materials [22–24]. The changes in composition and particle size observed here by annealing are expected. The SEM micrographs confirm the XRD results discussed above.

Fig. 2b–d shows that the annealed films, with larger sizes and more defined rod shapes, involve more pores hidden in between. The pores occur due to the random orientations of the rod shaped particles.

A closer look at Fig. 2 shows that the films annealed at 150 and 250 °C involve stacks of multi-layers of rods. The multi-layer stacking is not observed in case of 350 °C annealed film, which looks more compact with fewer pores. These observations explain the lower thickness (~38 nm) of the film annealed at 350 °C. In Fig. 2a, the films involved mixed particles with smaller sizes that penetrate through the available spaces showing no apparent pores in between.

When annealing temperature was increased to 450 °C, relatively smaller grains were observed with pores in between adjacent grains, Fig. 2e. Morphology changed to particles with irregular shapes and was different from morphologies of other films. Fig. 2e shows that the film involves inter-connected agglomerates each with ~100 nm or more in diameter. Each agglomerate involves a number of smaller particles with sizes ~10 nm in diameter. The XRD results, discussed above, confirm loss of Cu_2SnSe_3 and formation of SnO_2 and Cu_2Se phases by annealing at 450 °C. Loss of Cu observed here explains the low film thickness (~34 nm) for the film.

Table 1 – Values of XRD signal intensity ratio Cu_2SnSe_3 [(002)/(13-1)]/[ITO/glass] (004) for films annealed at different temperatures.

Annealing temperature (°C)	Value of ratio
Un-annealed	1.36
150	1.00
250	2.65
350	3.28
450	N/A

Energy dispersive X-Ray

Tables 2a and 2b shows values of average atomic% together with standard deviations and atomic% ratio, measured for films annealed at different temperatures, respectively. The atomic% data were analyzed by area scanning (1 μm × 1 μm) for 5 different points on each film. Both un-annealed and annealed films show homogeneous compositions with only acceptable standard deviation values. Lower Cu and higher tin and Se contents in the un-annealed film indicate that the film

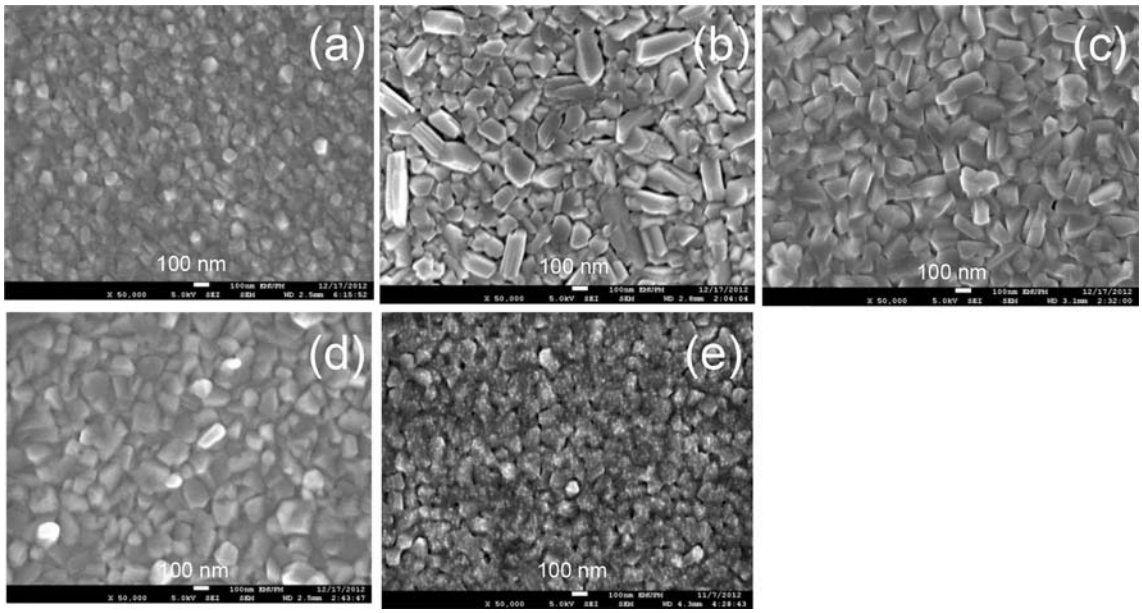

Fig. 2 – Surface morphology of films annealed at different temperatures (a) un-annealed, (b) 150, (c) 250, (d) 350 and (e) 450 °C. Scale bars are 100 nm.

Table 2a – Values of average and Std. Dev. of atomic % for different elements in different films.

Annealing temperature (°C)	Atomic % (Ave. of 5 points)			Standard deviation (5points)		
	Cu	Sn	Se	Cu	Sn	Se
Unannealed	17.76	25.08	57.16	0.40	0.20	0.26
150	34.03	11.41	54.57	0.44	0.32	0.51
250	35.25	10.85	53.90	0.48	0.36	0.50
350	35.72	10.96	53.32	0.37	0.14	0.24
450	17.39	24.71	57.89	0.68	0.72	0.73

Table 2b – Values of Atomic % ratio for different elements in films annealed at different temperatures.

Annealing temperature (°C)	Atomic % ratio	
	Cu/Se	Se/[Sn + Cu]
Unannealed	0.31	1.33
150	0.62	1.20
250	0.65	1.17
350	0.67	1.14
450	0.30	1.38

involved additional materials of SnSe and elemental Se. SEM images confirmed the presence of additional materials besides the Cu_2SnSe_3 phase, as discussed above. Higher copper contents are observed for films annealed at temperatures in the range 150–350 °C, which confirms the presence of Cu_2SnSe_3 in the annealed films as a dominant phase. Presence of SnSe cannot also be ruled out based on Tables 2a and 2b. Elemental Se, with its relatively low melting point of 217 °C [25] is expected to evaporate off under the annealing conditions. The presence of Cu_2SnSe_3 as a dominant phase in the films annealed at 150, 250 and 350 °C, as confirmed by EDX, XRD and SEM, allows sintering to occur between its particles. Sintering the particles causes growth in their sizes, as well documented by earlier reports for other materials [26,27]. The larger particle sizes observed for annealed films above are thus due to sintering. In the film annealed at 350 °C, sintering is more pronounced causing higher compactness and fewer pores, as discussed above by SEM. The results are also consistent with those shown in Table 1 where the 350 °C annealed film showed higher peak ratio than other counterparts.

As annealing temperature was increased to 450 °C, a decrease in copper content and an increase in relative Sn and Se contents were observed. This is due to possible decomposition of Cu_2SnSe_3 under the working conditions. Based on earlier TGA studies, the Cu_2SnSe_3 nano particles are known to exhibit stable structure at 250 °C and lower [28]. In a more recent report, Cu_2SnSe_3 films deposited by aerosol assisted chemical vapor deposition at 400 °C showed higher uniformity and better stoichiometry than films deposited at 450 °C [29]. Literature thus shows that the Cu_2SnSe_3 film may partially decompose at high temperatures such as 450 °C. As oxygen is included in trace amounts inside the nitrogen stream, and SnO_2 production is confirmed as discussed by XRD results above, partial decomposition of the Cu_2SnSe_3 phase is possible. EDX results further confirm the production of SnO_2 as shown in Tables 2a and 2b. The tin content increase is due to the formation of SnO_2 at the expense of Cu_2SnSe_3 compound decomposition in the film at 450 °C. The SnO_2 formation is due to presence of moisture, oxygen and carbon monoxide traces in the nitrogen stream, as explained above. Simple stoichiometric calculation for the total amount of passed nitrogen gas (assuming 99.999% pure, the remaining is moisture) in 30 min annealing shows that the total oxygen

content is ~0.1 × 10^{-6} mol. The film annealed at 350 °C (highest temperature below 450 °C) has dimensions of 1.0 cm × 1.0 cm × 38.2 nm. Assuming a density of 5.56 g/cm^3 [30], as the film has highest compactness as discussed above, the total mass of Cu_2SnSe_3 will then be ~0.636 × 10^{-6} g (~0.02 × 10^{-7} mol). Assuming incomplete reaction under equilibrium, then the amount of oxygen will be more than sufficient to cause partial (if not complete) consumption of the Cu_2SnSe_3 phase. Decomposition of Cu_2SnSe_3 under high temperature annealing under nitrogen is thus justified.

The characterization results observed here are consistent with those reported earlier. When Cu_2SnSe_3 was used as a source material to deposit the corresponding film electrodes by vacuum evaporation on ITO/glass substrates (at 300 °C), the film composition was readily controlled by careful control of the argon gas flow rate. Deposition at lower argon gas flow rate yielded Cu_2SnSe_3 films, whereas deposition under high argon gas flow rate (25 cm^3/min) yields SnSe as a dominant phase [20]. Collectively XRD, SEM and EDX results here show that annealing the authentically prepared Cu_2SnSe_3 at different temperatures under nitrogen affects the composition of the annealed film. Therefore films prepared under high argon gas flow rate involved SnSe as a major phase [20]. In this work the film prepared under the described working conditions involves Cu_2SnSe_3 phase mixed with SnSe and Se. When annealed under nitrogen in the range 150–350 °C, the Cu_2SnSe_3 became a major phase, while at 450 °C the film involved more of SnSe. Again the model discussed in earlier work [20] may successfully explain the loss of Cu from the film at 450 °C, since Cu is the element with lowest atomic mass. The results are thus consistent with those discussed earlier [20]. Moreover, the results are in agreement with earlier reports about stability of Cu_2SnSe_3 films ad discussed above [28,29].

Photoresponse

Fig. 3a and b shows PEC photoresponses with chopped light illumination under a linearly increased biased for the un-annealed and the 150 °C annealed film. Current is expected to change (increase/decrease) when the illumination is chopped (on and off) under cathodic bias (from 0.0 to −1.0 V vs Ag/AgCl). This is due to the carriers that are excited in the illumination region of the thin film and the excited minority carriers that diffuse to the surface during their lifetime to participate in an electrochemical reaction at the film/electrolyte interface. However, Fig. 3a and b shows that the un-annealed and the 150 °C annealed films exhibited no significant photoresponses. Other annealed films also showed same behavior indicating that even after annealing, the films have no significant photoresponse.

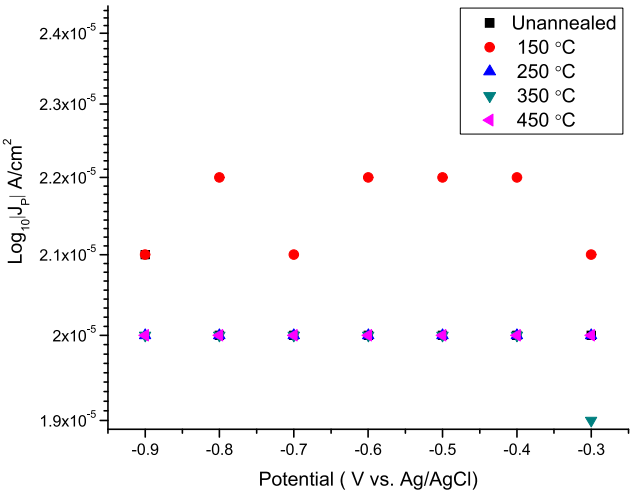

Fig. 4 – Plots of logarithmic absolute photocurrent vs. potential for film electrodes annealed at different temperatures.

Fig. 4 shows net values of photo current density vs. potential (J_P-V) plots, calculated by subtracting the dark current plots from corresponding photo current plots for films prepared at different annealing temperatures. The Y-axis shows logarithmic absolute photo current density $|J_p|$. The results show that annealing in the range 150–450 °C under argon gas atmosphere did not improve photoresponse. Annealing the deposited films increased the crystallinity of compounds but lead to formation of porosity between adjacent grains. Porosity is one possible reason for film internal resistance and

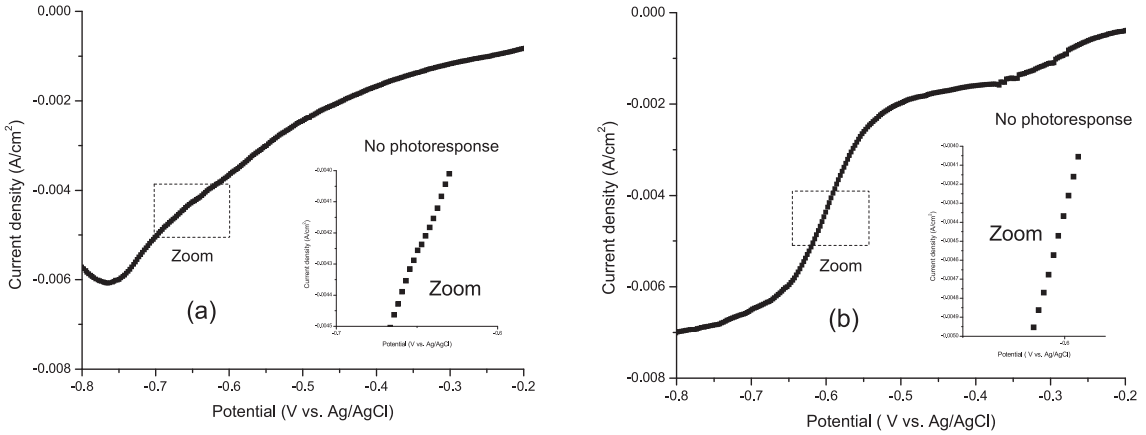

Fig. 3 – Photoresponse values for films deposited onto ITO/glass substrate under 5 cm^3/min at 300 °C a) un-annealed, b) annealed at 150 °C. Both films intermittently illuminated with a halogen lamp.

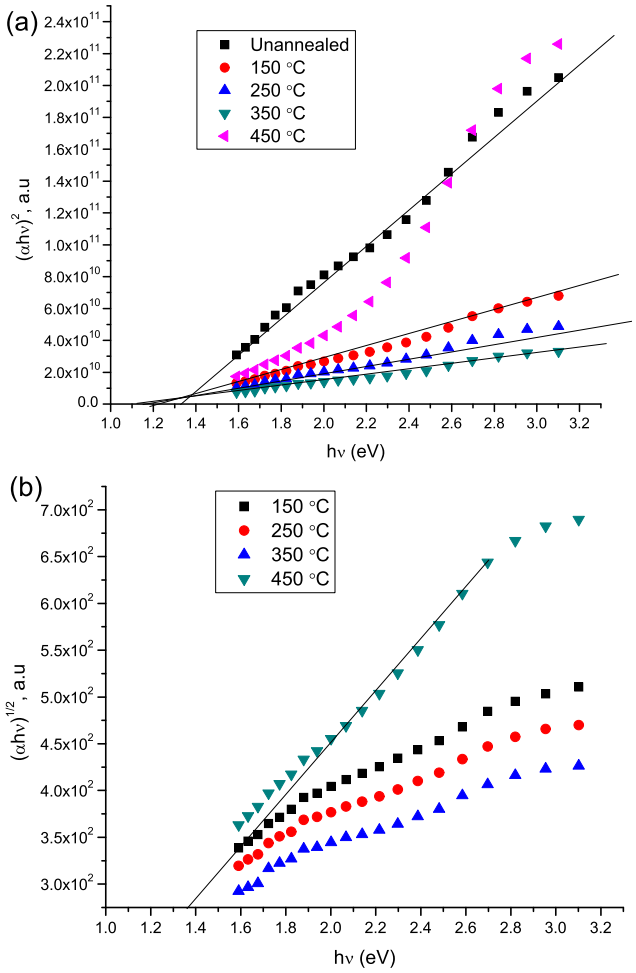

Fig. 5 – Plot of $(\alpha h\nu)^{2/n}$ vs: (a) $n = 1$ and (b) or $n = 4$ for CuSnSe films annealed at different temperatures.

poor charge transfer across the solid/redox couple interface. The film annealed at 450 °C involved mixed phases of SnO_2 and Cu_2Se, which is possibly responsible for increased internal film resistance and poor charge transfer across the solid/redox couple interface.

Optical properties

Effect of annealing on film electronic absorption spectra was studied in the range 400–800 nm. Fig. 5 shows plots of $(\alpha h\upsilon)^2$ vs. photon energy ($h\upsilon$) for all films, where α is the measured absorption coefficient calculated from the experimental value of absorbance (A) and measured thickness (t in nm unit) using the relation $\alpha = 2.303\ A/t$. The linearity in the relationship of $(\alpha h\upsilon)^2$ vs. ($h\upsilon$) for the films indicates that they all have direct band gaps.

Band gap energy values for film electrodes prepared from Cu_2SnSe_3 source under different annealing temperatures are summarized in Table 3. The measured direct band gap values 1.14–1.22 eV, respectively, Fig. 5a, for films annealed between 150 and 350 °C, are not far from literature value [31], which is 1.20 eV for Cu_2SnSe_3 film. The Table shows that the optical band gap decreased with increased annealing temperature. This is due to improved crystalline nature and increased particle sizes in the annealed films. The results are thus consistent with XRD and SEM results discussed above. The fact that band gap decreases after annealing was due to the increased order and particle size, in congruence with earlier literature for different systems [18,32–35]. For the film annealed at 450 °C the measured indirect band gap value was 1.37 eV. Indirect gap with higher value, 1.37 eV, compared to other films (with direct band gap) is due to the mixed Cu_2Se and SnO_2 compounds in the film.

Table 3 – Values of band gap energies for Cu_2SnSe_3 film electrodes annealed at different temperatures.

Annealing temperature (°C)	Band Gap (eV)
Unannealed	1.30
150	1.22
250	1.17
350	1.14
450	1.37

Conclusion

Authentic Cu_2SnSe_3 compound was used as a source to deposit films onto ITO/glass substrates (heated at 300 °C) by vacuum evaporation method under argon gas (flow rate 5 cm^3/min). Cu_2SnSe_3 mixed with SnSe as secondary phase, was observed for the un-annealed film. The prepared films were annealed at temperatures in the range 150–450 °C under nitrogen gas atmosphere. Annealing lowered photoresponse, and is therefore not recommended for photoresponse enhancement. Films annealed in the range 150–350 °C involved Cu_2SnSe_3 compound with relatively high crystallinity and particle sizes but exhibited more pores between adjacent grains, which is the reason for the lowered photoresponse. Optical band gap values for films annealed in the range 150–350 °C are comparable with known values for Cu_2SnSe_3. Annealing at higher temperature (450 °C) caused decomposition of Cu_2SnSe_3 and yielded a film with SnO_2 Cu_2Se, and SnSe. Porosity (in the films annealed at 150–350 °C) and mixed phases of SnO_2, Cu_2Se and Cu_2Se (in the film annealed at 450 °C) are responsible for increased internal film resistance and poor charge transfer across the solid/redox couple interface. As a result, poor photoresponse was observed for the annealed films.

Acknowledgment

Support donated by Grant Putra Inisiatif Putra Muda (GP-IPM/2015/9452000) of Universiti Putra Malaysia Grant Scheme is acknowledged.

REFERENCES

[1] Chung I, Kanatzidis MG. Metal chalcogenides: a rich source of nonlinear optical materials. Chem Mater 2013;26:849–69.
[2] Wang ZY, Zhang RJ, Lu HL, Chen X, Sun Y, Zhang Y, et al. The impact of thickness and thermal annealing on refractive index for aluminum oxide thin films deposited by atomic layer deposition. Nanoscale Res Lett 2015;10:1–6.
[3] Winzer A, Szabó N, Wachowiak A, Jordan PM, Heitmann J, Mikolajick T. Impact of postdeposition annealing upon film properties of atomic layer deposition-grown Al_2O_3 on GaN. J Vac Sci Technol B 2015;33. 01A106.
[4] Chuang CL, Chang MW, Chen NP, Pan CC, Liu CP. Improving performance of CIGS solar cells by annealing ITO thin films electrodes. Int J Photoenergy 2015;2015:8.
[5] Shiyani T, Patel M, Mukhopadhyay I, Ray A. Effect of Annealing on Structural Properties of Electrodeposited CZTS Thin Films. IETE Tech Rev 2016;33:2–6.
[6] Arasu PA, Williams RV. Effect of annealing temperature on structural and optical parameters of sol–gel routed molybdenum oxide thin film. Surf Rev Lett 2015;22. 1550054.
[7] Hilal HS, Salih SK, Sa'Adeddin IA, Campet G. Effect of annealing and of effect of annealing and of cooling rates on n-gaas electrode photoelectrochemical characteristics. Act Passiv Electron Compon 2004;27:69–80.
[8] Salih SK, Hilal HS, Sa'deddin IA, Sellier E, Campet G. Modification of n-Si characteristics by annealing and cooling at different rates. Act Passiv Electron Compon 2003;26:213–30.
[9] Portier J, Hilal HS, Saadeddin I, Hwang SJ, Subramanian MA, Campet G. Thermodynamic correlations and band gap calculations in metal oxides. Prog Solid State Chem 2004;32:207–17.
[10] Yunos MASM, Talib ZA, Yunus WMM, Sulaiman MYM, Chyi JLY, Paulus WS. X-ray diffraction analysis of thermally evaporated copper tin selenide thin films at different annealing temperature. J Sains Nukl Malays 2011;23:46–52.
[11] Surech Babu G, Kishore YB, Reddy YBK, Raja VS. Growth and characterization of Cu 2 SnSe 3 thin films. Mater Chem Phys 2006;96:442–6.
[12] Bhaskar PU, Babu GS, Kumar YBK, Raja VS. Investigations on co-evaporated Cu 2 SnSe 3 and Cu 2 SnSe 3–ZnSe thin films. Appl Surf Sci 2011;25:8529–34.
[13] Talib ZA, Yunus WM, Sulaiman MYM, Chyi JLY, Paulus WS. X-ray diffraction analysis of thermally evaporated copper tin selenide thin films at different annealing temperature. J Mater Sci Eng 2010;4:28–33.
[14] Sabli N, Talib ZA, Yunus WM, Zainal Z, Hilal HS, Fujii M. New technique for efficiency enhancement of film electrodes deposited by argon gas condensation from metal chalcogenide sources. Int J Electrochem Sci 2013;8:12038–50.
[15] Sabli N, Talib ZA, Yunus WMM, Zainal Z, Hilal HS, Fujii M. CuZnSnSe thin film electrodes prepared by vacuum evaporation: enhancement of surface morphology and photoelectrochemical characteristics by argon gas. Mater Sci Forum 2013;756:273–80.
[16] Santhanam KSV, Sharon M. Photoelectrochemical solar cells. New York, NY: Elsevier Science, Inc; 1988. p. 156–77.
[17] Fujii M, Kawai T, Kawai S. Photoelectrochemical properties of cadmium chalcogenide thin films prepared by vacuum evaporation. Sol Energy Mater 1988;18:23–35.
[18] Zyoud A, Saa'deddin I, Khudruj S, Hawash ZM, Park D-H, Campet G, et al. CdS/FTO thin film electrodes deposited by chemical bath deposition and by electrochemical deposition: a comparative assessment of photo-electrochemical characteristics. Solid State Sci 2013;18:83–90.
[19] Zyoud A, Saadeddin I, Khurduj S, Mari'e M, Hawash ZM, Campet G, et al. Combined electrochemical/chemical bath depositions to prepare CdS film electrodes with enhanced PEC characteristics. J Electroanal Chem 2013;707:117–21.
[20] Sabli N, Talib ZA, Yunus WMM, Zainal Z, Hilal HS, Fujii M. Film electrodes deposited from Cu_2SnSe_3 source in comparison with those deposited from SnSe and Cu 2 ZnSnSe 4 sources by thermal vacuum evaporation: effect of argon gas flow rate. Electrochim Acta 2014;139:238–43.
[21] Peck MA, Langell MA. Comparison of nanoscaled and bulk NiO structural and environmental characteristics by XRD, XAFS, and XPS. Chem Mater 2012;24:4483–90.
[22] Gupta A, Bhatti HS, Kumar D, Verma NK, Tandon RP. Nano and bulk crystals of ZnO: synthesis and characterization. Dig J Nanomater Biostructures 2006;1:1–9.
[23] Noack V, Eychmuller A. Annealing of nanometer-sized zinc oxide particles. Chem Mater 2002;14:1411–7.
[24] Xu XN, Wolfus Y, Shaulov A, Yeshurun Y, Felner I, Nowik I, et al. Annealing study of Fe2O3 nanoparticles: magnetic size effects and phase transformations. J Appl Phys 2002;9:4611–6.
[25] http://www.acialloys.com/wp-content/uploads/msds/se.html (accessed March 2016).
[26] Volkman SK, Yin S, Bakhishev T, Puntambekar K, Subramanian V, Toney MF. Mechanistic studies on sintering of silver nanoparticles. Chem Mater 2011;23:4634–40.
[27] Nahar M, Becker MF, Keto JW, Kovar D. Highly conductive nanoparticulate films achieved at low sintering temperatures. J Electron Mater 2015;44:2559–65.
[28] Chyi JLY, Talib ZA, Mahmood W, Yunus M, Zainal Z. Preparation and thermal stability characterization of copper tin selenide semiconductor nanoparticles. Mater Sci Forum 2013;756:66–73.
[29] Kevin P, Malik SN, Malik MA, O'Brien P. The aerosol assisted chemical vapour deposition of SnSe and Cu 2 SnSe 3 thin films from molecular precursors. Chem Commun 2014;50:14328–30.
[30] https://www.citrination.com/uploads/1864/samples/cu-_-2-snse-_-3-density-crystal-system (Accessed March 2016).
[31] Zainal Z, Kassim A, Hussein MZ, Ching CH. Effect of bath temperature on the electrodeposition of copper tin selenide films from aqueous solution. Mater Lett 2004;58:2199–202.
[32] Lippens PE, Lannoo M. Calculation of the band gap for small CdS and ZnS crystallites. Phys Rev B 1989;39:10935–42.
[33] Banerjee R, Jayakrishnan R, Banerjee R, Ayyub P. Effect of the size-induced structural transformation on the band gap in CdS nanoparticles. J Phys Cond Matt 2000;12. 10647.
[34] Hilal HS, Ismail RMA, El-Hamouz A, Zyoud A, Saadeddin I. Effect of cooling rate of pre-annealed CdS thin film electrodes prepared by chemical bath deposition: enhancement of photoelectrochemical characteristics. Electrochim Acta 2009;54:3433–40.
[35] Chavhan SD, Senthularasu S, Lee SH. Annealing effect on the structural and optical properties of a $Cd_{1-x}Zn_xS$ thin film for photovoltaic applications. Appl Surf Sci 2008;254:4539–45.